

# Numerical simulation of the influence of wind speed on asphalt fume diffusion concentration distribution in road construction

Xiaobo Guo

(School of Management/ Shanghai University, Shanghai)

---

**ABSTRACT:** In the construction of the asphalt pavement, the asphalt will easily release a large amount of asphalt fume when heated. Asphalt fume has been recognized as a toxic and harmful substance at home and abroad. This paper takes asphalt fume as the research object, and conducts a dynamic analysis study on the influence of wind speed on its diffusion concentration during the construction process. The simulation model is established by using fluid mechanics simulation software Fluent, and the effectiveness of model is verified based on the field measured data and experimental simulation results. Under the conditions of only changing the wind speed to 2.5m/s, 6m/s, and 10m/s, it is found that as the wind speed increases, the peak concentration of asphalt fume will appear in advance, and the increase in wind speed is more conducive to the diffusion of asphalt fume. The research results will be of reference significance of road construction pollutant emission analysis and construction worker health management.

**KEYWORDS** -Asphalt fume, Fluent, Numerical simulation, Road Construction

---

Date of Submission: 07-11-2020

Date of Acceptance: 20-11-2020

---

## I. INTRODUCTION

In recent years, China's road construction projects have advanced by leaps and bounds. In 2018 alone, the total kilometer mileage has exceeded 4.77 million kilometers [1]. In the actual construction process of asphalt pavement, construction workers will directly come into contact with asphalt or inhale the asphalt fume emitted by asphalt, which will pose a threat to their health. In particular, asphalt materials often need to be heated during the construction process, exposing workers to an environment full of asphalt fume [2]. Asphalt fumes is easy to cause air pollution and occupational diseases of construction workers, and it has been recognized as one of the most significant factors causing occupational damage to highway construction workers [3].

At present, many scholars have carried out relevant numerical simulation research on the environmental field of asphalt road engineering. In the simulation study of asphalt heat emission of the paving process of tunnel asphalt pavement, Zhou Linghao found that the problem of excessively high temperature in the construction environment of tunnel asphalt pavement can be effectively solved by ventilating the construction area [4]. Zhao Tianyan et al took the bituminous smoke emission source as the research object, and used laboratory simulation experiments to solve the difficulty of the low-temperature and high-temperature storage tank that the free-emission rate of bitumen smoke was too low and difficult to test [5]. However, there are few researches on the simulation of asphalt fume concentration diffusion at this stage. Therefore, this paper simulates the change of asphalt fume concentration diffusion during asphalt road construction and considers the influence of wind speed changes on its diffusion concentration.

## II. MODEL ESTABLISHMENT

### 2.1 Fluent introduction

Fluent software is currently the mainstream fluid mechanics simulation software in the world. It has advanced numerical methods and powerful pre-processing functions. It can calculate physical models such as compressible and incompressible fluids, multiphase flow, chemical combustion, etc. It is suitable for this article. Research content and the following content will be analyzed using Fluent19.0 version.

### 2.2 Governing equation

#### 2.2.1 Mass conservation equation

The mass conservation equation is also called the continuity equation. This equation indicates that the mass of fluid flowing in and the mass flowing out of fluid per unit times are equal.

$$(1) \frac{\partial \rho}{\partial t} + \frac{\partial(\rho u_x)}{\partial x} + \frac{\partial(\rho u_y)}{\partial y} + \frac{\partial(\rho u_z)}{\partial z} = S_m$$

Where  $\rho$  is the fluid density,  $\text{kg/m}^3$ ;  $t$  represents time,  $s$ ;  $u_x$  represents the velocity component of the fluid on the X axis,  $\text{m/s}$ ;  $u_y$  represents the fluid velocity on the Y axis,  $\text{m/s}$ ;  $u_z$  represents the velocity component on the Z axis,  $\text{m/s}$ ; the source term  $S_m$  represents the mass of other items added to the continuous phase,  $\text{kg/m}^3\cdot\text{s}$ .

### 2.2.2 Momentum conservation equation

$$(2) \begin{cases} \frac{\partial}{\partial t}(\rho u_x) + \frac{\partial}{\partial x}(\rho u_x u_x + \rho u_x u_y + \rho u_x u_z) = \frac{\partial p}{\partial x} + \frac{\partial \tau_{xx}}{\partial x} + \frac{\partial \tau_{yx}}{\partial y} + \frac{\partial \tau_{zx}}{\partial z} + \rho g_x + F_x \\ \frac{\partial}{\partial t}(\rho u_y) + \frac{\partial}{\partial y}(\rho u_y u_x + \rho u_y u_y + \rho u_y u_z) = \frac{\partial p}{\partial y} + \frac{\partial \tau_{xy}}{\partial x} + \frac{\partial \tau_{yy}}{\partial y} + \frac{\partial \tau_{zy}}{\partial z} + \rho g_y + F_y \\ \frac{\partial}{\partial t}(\rho u_z) + \frac{\partial}{\partial z}(\rho u_z u_x + \rho u_z u_y + \rho u_z u_z) = \frac{\partial p}{\partial z} + \frac{\partial \tau_{xz}}{\partial x} + \frac{\partial \tau_{yz}}{\partial y} + \frac{\partial \tau_{zz}}{\partial z} + \rho g_z + F_z \end{cases}$$

Where  $p$  is the static pressure;  $\tau$  is the stress tensor;  $g$  and  $F$  are the gravitational volume force and the external volume force, respectively, and  $F$  contains other model related source terms [6].

The stress tensor gives the following formula:

$$(3) \tau_{ij} = \left[ u \left( \frac{\partial u_i}{\partial x_j} + \frac{\partial u_j}{\partial x_i} \right) \right] - \frac{2}{3} \mu \frac{\partial u_l}{\partial x_l} \delta_{ij}$$

### 2.2.3 Energy conservation equation

A flow field system containing heat exchange must satisfy an energy conservation equation, which is based on the first law of thermodynamics. It's expressed as the rate of increase in the energy of the system is equal to the net heat flow plus the work done on the object by the volume force and the surface force.

$$(4) \frac{\partial(\rho T)}{\partial t} + \text{div}(p u T) = \text{div} \left( \frac{k}{c_p} \text{grad} T \right) + S_T$$

Where,  $c_p$  is the specific heat capacity,  $\text{W}/(\text{kg}\cdot\text{K})$ ;  $T$  is temperature;  $K$  is the heat transfer coefficient of the fluid;  $S_T$  is the internal heat source of the fluid and the part where the fluid's mechanical energy is converted into heat energy due to the action of viscosity, also known as viscous dissipation term,  $\text{W/m}^3$ .

### 2.2.4 Standard k-ε turbulence model

This paper adopted the two-equation standard k-ε turbulence model. The standard k-ε turbulence model was first proposed by Launder and Spalding. By introducing the turbulent dissipation rate  $\varepsilon$  equation on the basis of the turbulent kinetic energy  $k$  equation, and then using the calculation results of  $k$  and  $\varepsilon$  to calculate the turbulent viscosity, the Reynolds stress solution was obtained.

Turbulence energy  $k$  equation:

$$(5) \frac{\partial}{\partial t}(\rho k) + \frac{\partial}{\partial x_i}(\rho k \mu_i) = \frac{\partial}{\partial x_j} \left[ \left( u + \frac{\mu_i}{\sigma_k} \right) \frac{\partial k}{\partial x_j} \right] + G_k + G_b - \rho \varepsilon - Y_m + S_k$$

Turbulent dissipation rate  $\varepsilon$  equation:

$$(6) \frac{\partial}{\partial t}(\rho \varepsilon) + \frac{\partial}{\partial x_j}(\rho \varepsilon \mu_i) = \frac{\partial}{\partial x_j} \left[ \left( \mu + \frac{\mu_i}{\sigma_\varepsilon} \right) \frac{\partial \varepsilon}{\partial x_j} \right] + C_{1\varepsilon} \frac{\varepsilon}{k} (G_k + C_{3\varepsilon} G_b) - C_{2\varepsilon} \rho \frac{\varepsilon^2}{k} + S_\varepsilon$$

In the formula,  $G_k$  is the turbulent kinetic energy caused by laminar flow velocity gradient;  $G_b$  is the turbulent kinetic energy caused by buoyancy;  $Y_m$  is the utility caused by compressible flow diffusion;  $C_{1\varepsilon}, C_{2\varepsilon}, C_{3\varepsilon}$  are model constants, with values of 1.44, 1.92 and 0.09 respectively;  $\sigma_k$  and  $\sigma_\varepsilon$  are the turbulent Prandtl numbers of the  $k$  equation and the  $\varepsilon$  equation, taking the values 1.0 and 1.3, respectively;  $\mu_i$  is the turbulent flow velocity which can be determined by the following formula, and  $C_u$  is a constant value of 0.09[7]:

$$(7) \mu_i = \rho C_u \frac{k^2}{\varepsilon}$$

### 2.2.5 Discrete phase model

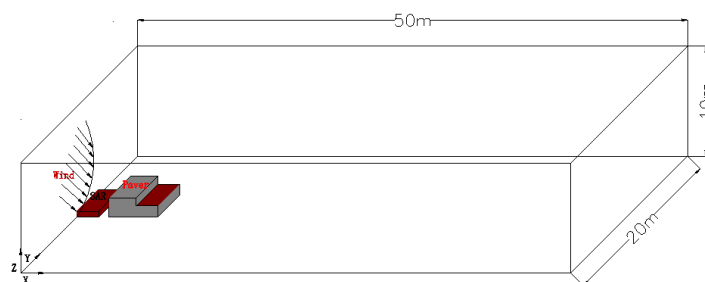
When there are two substances in the flow field, gas and solid, it is the motion of gas-solid two-phase flow. Gas-solid two-phase flows contains three physical models, namely the discrete phase model, the continuum model and the fluid pseudo-particle model [8][9]. The discrete phase model assumes that there is a very rare phase, and the interaction between particles can be ignored. This type of model regards particles as a discrete phase and gas as a continuous phase. By considering the interaction between particles and between particles and gas Function to simulate the movement trajectory of particles.

In this study, because the concentration of asphalt fume particles of the flow field is low, and the interaction between particles can be ignored, this study adopted the Discrete Phase Model (DPM) for numerical simulation, and the Euler method is used to solve the continuous Phase.

### 2.3 Geometry model and meshing

During the construction of asphalt roads, the source of asphalt fume emission mainly came from the asphalt pavement and paver. Combined with the actual situation of the construction site, a physical model was established. The model includes: calculation domain, asphalt pavement and paver. The calculation domain was a large cuboid with a length of 50m, a width of 20 meters, and a height of 10 meters and the asphalt pavement was 2.8 meters wide and 0.05 meters thick. In order to facilitate the establishment of the physical model, the paver was simplified into a rectangular shape with a height of 1.7 meters and a length of 4.5 meters. Through field measurement, both the paver and the asphalt pavement were spread forward at a speed of 0.15m/s. The release source of asphalt fume came from the asphalt pavement and the paver hopper. On-site, the experimental personnel hold portable aerosol detectors to detect the on-site concentration, and set the monitoring points in the model to correspond to the actual measurement points. The detailed geometric model is shown in Fig. 1.

**Figure 1 Physical model of asphalt road construction simulation**



There were many kinds of object movement problems in the road construction process. In this study, the asphalt pavement and the paver were moving objects, and both were paving forward at a speed of 0.15m/s, in order to simulate the problem, this article first used ICEM to mesh the physical model, and then used dynamic mesh technology to solve the boundary motion problem of the fluid domain. By loading the transient Profile file, the linear motion of the paver and the deformation of the asphalt pavement was specified and used Layering method to update the grid.

### 2.4 Boundary conditions

In this simulation calculation, the setting of boundary conditions included the setting of dust particles, air velocity inlet, pressure outlet, wall conditions, etc.

Dust particulate matters setting: This study used a fluid-solid coupling model. The release source was asphalt pavement and paver hopper, and the released pollutant was asphalt fume particulate matter. Particles were sprayed by a surface source. In the simulation, a total of 160 spray points were set for the initial surface source, the speed was 1m/s, the temperature was 150°C. The boundary conditions of the entrance and exit were set to Escape, and the remaining walls were Reflect.

Air speed inlet and pressure outlet: Asphalt pavement construction was an outdoor operation. The measured temperature on site was 32.9°C, and the wind speed was 0.5m/s. The inlet and outlet of the calculation domain was connected to the atmosphere, and the external pressure at the outlet was atmospheric pressure.

Wall surface conditions: except for the ground, the wall surface was set as a constant temperature non-slip wall surface.

### III. RESULTS AND ANALYSIS

#### 3.1 Numerical simulation verification

Fig.2 shows the comparison between the numerical simulation results and the field experimental data. It can be seen from the figure that the simulated data was in good agreement with the experimental data, and the model has a good degree of fit, but the experimental data concentration and fluctuates range are significantly higher than the numerical simulation concentration. Combining various factors such as construction site conditions, the reasons for the analysis deviation may come from experimental conditions, accuracy of measuring instruments, etc. There are multiple sources of interference in the actual construction site, such as exhaust emissions from large-scale machinery and equipment and disturbances from surrounding workers. In the actual measurement process, the wind speed and wind temperature are dynamically changing, but in the numerical simulation, the wind speed and wind temperature are constant, which will cause errors in the experiment.

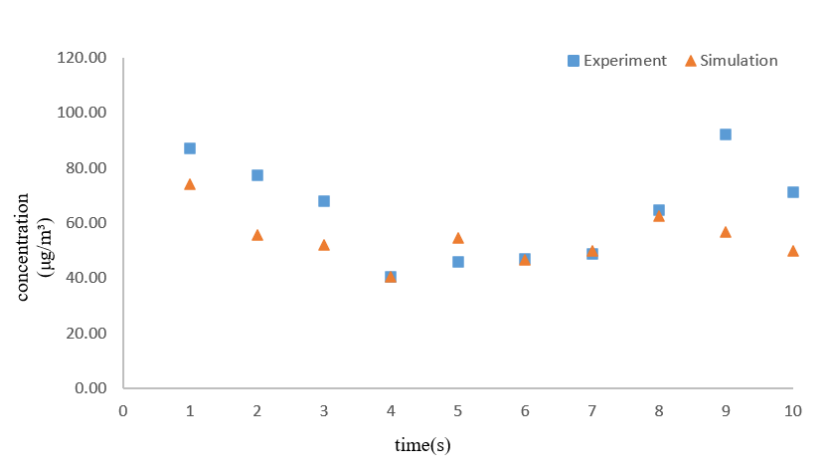


Figure 2 Comparison of simulated data and test data

#### 3.2 The influence of wind speed on the diffusion concentration of asphalt fume

Two detection points are set at different locations in the model, and observe the concentration changes at the two monitoring points by changing the numerical simulation wind speed changes. The results are shown in Fig.3-4. By comparing the concentration changes in Fig. 3, we can find that: When the wind speed is 2.5m/s, monitoring point 1 reaches the highest concentration point of 37.94µg/m³ in the 6th second. When the wind speed is 6.5m/s, monitoring point 1 reaches the highest concentration point of 11.93µg/m³ in the fourth second. When the wind speed is 10m/s, the monitoring point 1 reaches the highest concentration point 2µg/m³ in the third second, which indicates that as the wind speed increases, the peak of the asphalt fume concentration will appear earlier, and the greater the wind speed, the more beneficial the diffusion of asphalt fume.

Comparing with Fig.3-4, it can be found that (monitoring point 1 is located at the lower air outlet of monitoring point 2) when the wind speed is less than 2.5m/s, the asphalt fume concentration at measurement point 1 is significantly higher than that measurement point 2. When the wind speed increases to 6.5m/s, the difference between the overall concentration of measuring point 2 and measuring point 1 becomes smaller, but it is still higher than the concentration of measuring point 1. When the wind speed increases to 10m/s, measuring point 1 is almost the same as the asphalt fume concentration of measuring point 2. It can be seen that when the wind speed increases to a certain level, the asphalt fume concentration at each point tends to be the same. As shown in Fig. 3 and 4, when the wind speed increases to 10m/s, the pollutants the concentration will not change with distance. In addition, the peak concentration of measurement point 1 is higher than the peak concentration of measurement point 2, which indicates that the cumulative effect of pollutants' environmental pollution has occurred at the downwind monitoring point 1. As the paver is running, the asphalt fume released from the road is accumulated to the next monitoring point, but the wind speed increases to a certain level, this accumulation is no longer obvious.

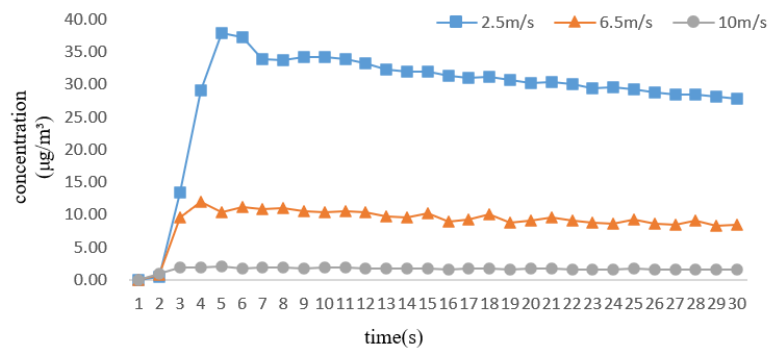


Figure 3 Concentration change curve of monitoring point 1

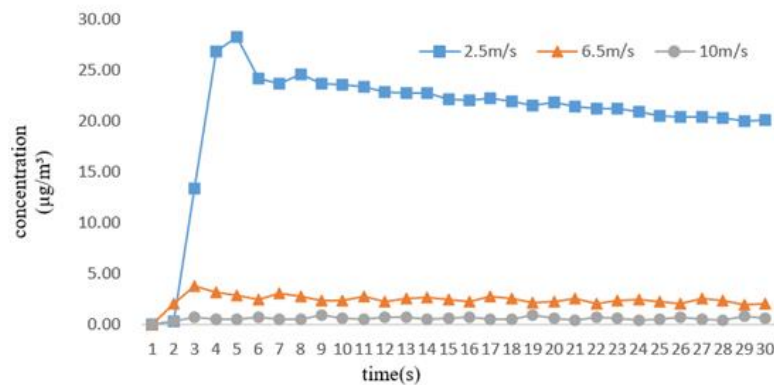


Figure 4 Concentration change curve of monitoring point 2

#### IV. CONCLUSION

Through the numerical simulation of the asphalt fume concentration during the road construction process, the following main conclusions are drawn. Under the influence of different wind speeds, as the wind speed increases, the peak value of the asphalt fume concentration will appear in advance, and when the wind speed increases to a certain level, The concentration of asphalt fume at each point tends to be the same; when the wind speed is small, the cumulative effect of asphalt fume will appear at the downwind. When the wind speed is high, it is more conducive to the diffusion of asphalt fume, and this accumulation will no longer be obvious.

#### ACKNOWLEDGEMENTS

Thanks to Hou Hui for her contribution to analysis in this paper, thanks to everyone involved in data collection, and thanks to the support of the Project in Shanghai area.

#### REFERENCES

- [1]. Ministry of Transport, 2018, 2017 Statistical Bulletin on the Development of the Transport Industry.
- [2]. Chong D, Wang Y, Zhao K, et al. Asphalt fume exposures by pavement construction workers, Current status and project cases, Journal of Construction Engineering and Management, 2018, 144(4): 05018002.
- [3]. Asphalt Institute and Eurobitume, The bitumen industry-A global perspective (third edition), 2015, <[http://www.asphaltinstitute.org/wp-content/uploads/IS230\\_3rdedition.pdf](http://www.asphaltinstitute.org/wp-content/uploads/IS230_3rdedition.pdf)> (Feb. 17, 217).
- [4]. L.H. Zhou, Numerical simulation of environmental field in highway tunnel, master's thesis, Chang'an University, Xian, Shanxi,2012.
- [5]. T.Y. Zhao, H.J. Whang, H. Du and Z. Dong, A Simulation Experiment on Asphalt Smoke Emission Source and Cost-benefit Analysis for Its Control Equipment, Journal of Wuhan University of Technology (Transportation Science & Engineering),2005(01):41-44.
- [6]. Q.N. Pan, Numerical simulation on Indoor Hydrothermal Environment and Particle Matter of the Piggery, master's thesis, Zhejiang University, Hangzhou, Zhejiang ,2016.
- [7]. M.M. Meng, Numerical Simulation of Emissions (CO) by Rubber Tire Vehicle in Xiegou Coal Mine, master's thesis, Taiyuan University of Technology, Taiyuan, Shanxi, 2016.
- [8]. Bolio E J, Yasuna J A, Sinclair J L, Dilute turbulent gas-solid flow in risers with particle-particle interactions, International Journal of Multiphase Flow, 1996, 22(S1): 94-94.
- [9]. X.M. Rui. Theory and calculation of gas-solid multiphase flow in engineering, Journal of Chinese Society of Power Engineering,1990(06):38.